

Article

Production of Substitute Natural Gas Integrated with Allam Cycle for Power Generation

Daniele Candelaresi ^{1,2}  and Giuseppe Spazzafumo ^{1,2,*}

¹ Department of Civil and Mechanical Engineering, University of Cassino and Southern Lazio, 03043 Cassino, Italy

² Energy Transition Team (EnTraT srls) Academic Spin-Off of University of Cassino and Southern Lazio, 03043 Cassino, Italy

* Correspondence: spazzafumo@unicas.it

Abstract: The accumulation of energy from non-programmable renewable sources is a crucial aspect for the energy transition. Using surplus electricity from renewable energy sources, power-to-gas plants allow to produce a substitute natural gas (SNG) that can be injected in the existing infrastructure for large-scale and long-term energy storage, contributing to gas grid decarbonisation. The plant layout, the method used for carbon dioxide capture and the possible cogeneration of electricity can increase the efficiency and convenience of SNG synthesis plants. In this work, a system for the simultaneous production of SNG and electricity starting from biomass and fluctuating electricity from renewables is proposed, using a plant based on the Allam thermodynamic cycle as the power unit. The Allam power cycle uses supercritical CO₂ as evolving fluid and is based on the oxycombustion of gaseous fuels, thus greatly simplifying CO₂ capture. In the proposed system, oxycombustion is performed using biomass syngas and electrolytic oxygen. The CO₂ generated by means of oxycombustion is captured, and it is subsequently used together with renewable hydrogen for the production of SNG through thermochemical methanation. The system is also coupled with a solid oxide electrolyser and a biomass gasifier. The whole plant was analysed from an energy-related point of view. The results show overall plant efficiency of 67.6% on an LHV basis (71.6% on an HHV basis) and the simultaneous production of significant amounts of electricity and of high-calorific-value SNG, whose composition could be compatible with the existing natural gas network.

Keywords: Allam cycle; biomass; SNG; power to gas; electrolysis; methanation; CCUS; oxycombustion



Citation: Candelaresi, D.; Spazzafumo, G. Production of Substitute Natural Gas Integrated with Allam Cycle for Power Generation. *Energies* **2023**, *16*, 2162. <https://doi.org/10.3390/en16052162>

Academic Editors: Kegong Fang, Gangli Zhu, Ying Yang and Shenghua Liu

Received: 11 January 2023

Revised: 13 February 2023

Accepted: 20 February 2023

Published: 23 February 2023



Copyright: © 2023 by the authors. Licensee MDPI, Basel, Switzerland. This article is an open access article distributed under the terms and conditions of the Creative Commons Attribution (CC BY) license (<https://creativecommons.org/licenses/by/4.0/>).

1. Introduction

Nowadays, the debate on energy and environmental issues has gained significant importance, not only within the scientific community, but also at political and industrial levels. Despite the variety of environmental issues related to human activity, most of the media attention is mainly paid to climate change, which in turn manifests as global warming and extreme weather events and which is perceived as one of the greatest problems of humanity, to be solved as soon as possible [1,2]. For this reason, the energy transition towards clean and reliable energy systems is being advocated by many sides, and recent years have seen the flourishing of several goals in this sense [3–5]. Indeed, climate change is intimately related to energy issues. According to a large part of the scientific community, the main cause of these climatic changes lies in the sharp increase in CO₂ and other greenhouse-gas (GHG) concentrations in the atmosphere compared with pre-industrial times due to man’s massive use of fossil fuels for energy purposes [6,7]. Currently, annual GHG emissions amount to around 50 billion tonnes of equivalent carbon dioxide (CO₂eq), of which around three-quarters come from the energy sector [8,9]. According to the International Energy Agency, in the year 2021, the overall energy-related global GHG emissions reached a new record of 40.8 Gt of CO₂eq, where the 89% of this amount consisted

of CO₂ emissions from combustion for energy purposes and industrial processes [10]. Regarding the electricity generation sector alone, its global CO₂ emissions amounted to 13 Gt in 2021, or over one-third of all CO₂ emissions related to the energy sector. However, despite the recent increase in the demand for electricity, the rapid expansion of renewable sources such as solar photovoltaic and wind power is beginning to stem the growth in GHG emissions [11]. Renewable energy sources (RESs), which do not involve direct carbon emissions, are seen as one of the most promising solutions to solve the problem of global warming [12,13]; however, the typical randomness and non-programmability of some of these sources (such as wind and solar power) poses various obstacles to this energy transition [14–16]. For this reason, energy storage systems are essential to overcome these barriers and increase the penetration of renewable sources in the energy mix, both not to jeopardise the stability of the electricity grid and to decouple the production of energy from its demand and manage the surplus energy [17–19].

Among the energy storage techniques, chemical storage (i.e., storage into the chemical bonds of a molecule), stands out for its energy density and versatility. In particular, the power-to-fuel (P2f) technique allows hydrogen or synthetic fuels to be produced using the surplus of electricity production from RESs, enabling energy to be stored on a large scale and for a long time (from days up to seasons) [18–22]. In addition, the P2f technique helps to avoid energy curtailment and can offer stabilization services to the electricity grid. The produced fuels can be stored more easily than electricity and then be used to replace fossil fuels, also allowing the decarbonization of hard-to-abate sectors where electrification is not possible or not convenient to be achieved, a concept also known as power-to-X [22–25]. Hydrogen is the simplest fuel that can be produced by means of P2f, starting from water and electricity, that is used to power an electrolyser and split the water molecule into hydrogen and oxygen. Hydrogen is a clean fuel, as it produces no direct carbon emissions during its use, and its environmental sustainability is even better when produced from a surplus of renewable electricity [26]. However, hydrogen storage and distribution still face several hurdles before they can achieve large-scale application, as a dedicated hydrogen infrastructure is still missing. A first option to overcome these barriers could be the direct injection of hydrogen into existing natural gas pipelines [27,28]. Recently, Italian gas grid operator SNAM successfully carried out two tests, blending natural gas with 5%_{vol} hydrogen in the first case and with 10%_{vol} hydrogen in the second one [29]. However, the amount of hydrogen that can be injected in the grid is limited for both safety issues and changes in the characteristics of the fuel supplied. Therefore, an alternative option is hydrogen conversion into chemicals or fuels that can be managed and distributed in an easier way. One of the most promising fuels in this sense is substitute natural gas (SNG); taking advantage of the capillarity and the extension of the natural gas distribution network, SNG mainly consisting of methane could be directly injected into the grid, representing a good solution in the short term and favouring the transition to pure hydrogen in the long term [20,30,31].

The production of SNG requires the availability of hydrogen and carbon, where the latter can be obtained from several sources. In P2f systems, therefore, the electrolysers for renewable hydrogen production are often coupled with carbon capture utilisation and storage (CCUS) systems. The latter usually make it possible to capture CO₂ that can be further used within a chemical reactor together with (renewable) hydrogen for subsequent conversion to fuels or chemicals. When it comes to synthetic fuels, the carbon source is essential to determining the environmental sustainability of the final product [32]. Fossil-based carbon dioxide can be captured in a concentrated form from industrial sources; however, cleaner fuel can be obtained when the carbon source is biomass or waste materials. Biomass can make its carbon content available in several ways, depending on the type of biomass and the process used to elaborate it. Through the gasification process, lignocellulosic biomass can be converted into an easily usable combustible gas (called syngas) mainly composed of hydrogen and carbon oxides. On the other hand, anaerobic digestion is suitable for humid biomass and produces biogas mainly composed of methane and carbon dioxide.

One of the main disadvantages of common CCUS systems lies in the great energy consumption required to separate and capture carbon dioxide from the rest of the gases and for sorbents regeneration. This is particularly true for CO₂ direct air capture, while capture from industrial sources is less energy intensive, as the energy consumption is related to the carbon dioxide concentration in the gas [22]. In order to obtain energy, environmental and possibly also economic convenience, it is, therefore, essential to investigate CO₂ capture processes that consume as little energy as possible. In this regard, the oxycombustion of a carbon-containing fuel is one of the methods that can greatly simplify the process of CO₂ separation and capture, as oxycombustion allows to obtain mainly carbon dioxide and water vapour as final products in exhaust gases, where water can be easily separated by condensation [33,34]. Oxycombustion can be also used for syngas obtained by means of biomass gasification, and the derived exhaust gas is almost exclusively composed of carbon dioxide and steam, with trace amounts of other substances. The same could apply to biogas produced by means of anaerobic digestion, almost exclusively composed of methane and carbon dioxide. Furthermore, at the same time, the oxycombustion of a fuel allows electricity to be produced with better programmability and continuity than renewable sources. Finally, in the case of a plant equipped with an electrolyser, oxycombustion allows the electrolytic oxygen produced to be valorised.

This paper, therefore, proposes a system that cogenerates SNG and electricity starting from biomass and electricity surplus from RESs. This system is to be intended as an integrated energy storage system that allows to increase the flexibility and interconnection of the gas network and the electricity network. As a power-to-gas system, the proposed system can act as a bridge that connects the electricity grid and the gas grid. By accepting storable chemicals produced starting from excess electricity, the gas grid can act as a huge energy storage pool, helping to achieve electricity grid balancing and the match between electricity demand and production. The produced SNG can be injected into the gas grid, thus also enabling the seasonal or annual balancing of the overall energy system. Moreover, if the various reactants are stored in suitable tanks, electricity could be produced by the power plant in a more programmable and flexible way than electricity from variable RESs. The proposed integrated system, therefore, consists of: (i) an electrolyser powered by renewable electricity, (ii) a biomass processing system (lignocellulosic biomass gasification), (iii) a power unit based on oxycombustion that allows the production of electricity and simultaneous CO₂ sequestration to be achieved and (iv) a thermochemical methanation system for the production of SNG.

Figure 1 depicts a conceptual scheme of the proposed system. Electricity from RESs and water are fed to an electrolyser, which, thanks to an electrochemical reaction, splits water into hydrogen and oxygen. Biomass is sent to a gasifier together with a part of the oxygen produced by the electrolyser, since oxygen is used as a gasifying agent. In the gasifier, the solid biomass undergoes thermal degradation, which converts it into a gaseous fuel called syngas, which is mainly composed of carbon monoxide and hydrogen, with lower contents of other gaseous substances. Syngas coming from the biomass gasifier is fed to a power plant based on oxycombustion together with a part of the oxygen produced by the electrolyser. The power plant produces electric power and, at the same time, makes it possible to easily capture the carbon dioxide produced by means of oxycombustion. The carbon dioxide captured from the power plant is sent to a Sabatier process together with the hydrogen produced by the electrolyser. Here, carbon dioxide and hydrogen react together according to the methanation reactions to produce raw SNG mainly composed of methane and water. Finally, the raw SNG is upgraded by removing water via condensation, in order to obtain SNG with high calorific value. Overall, electric power surplus from variable RESs, water and biomass enter the system boundaries, while SNG and net electric power exit from the system. SNG and stable electric power can then be injected in their respective gas and electricity grids.

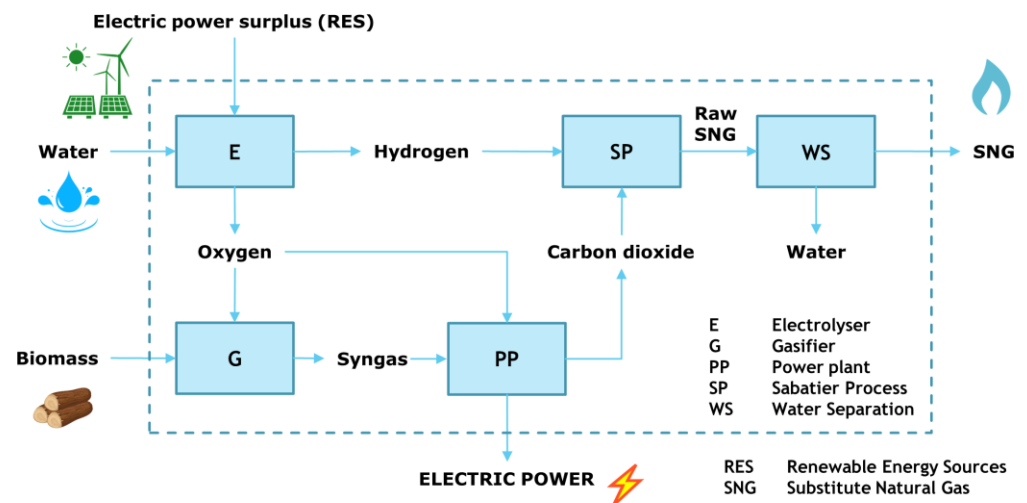


Figure 1. Simplified scheme of the proposed system.

A system such as the one shown in Figure 1 has been analysed in previous articles, where a gas turbine, a steam-injected gas turbine, an internal combustion engine and a high-temperature fuel cell were considered as alternative power units [35–37]. The same systems have also been analysed from an environmental impact point of view to evaluate the sustainability of the SNG produced [38]. The goal of such a system is to co-generate electricity and a renewable fuel, starting from biomass and the surplus of electricity from renewable sources. The main novelty on this article then, is that a plant based on the Allam thermodynamic cycle is considered as the power unit.

2. Allam Cycle

The Allam cycle, also known as NET Power cycle, was first patented in 2011 [39] and subsequently updated by the same authors [40–44]. This innovative thermodynamic cycle is similar to a high-pressure Brayton cycle, but uses CO₂ under supercritical conditions as the main evolving fluid, and it is based on the oxycombustion of a gaseous fuel to obtain heat addition within the fluid itself. The cycle was initially thought for the combustion of syngas obtained from coal gasification, and later, the use of natural gas was also considered [43]. However, it seems that only few literature studies have coupled the Allam cycle with a biomass gasifier or with an electrolyser for oxygen demand.

The conventional Allam cycle is shown in Figure 2 and described below.

To provide the oxygen needed for oxycombustion, the starting point of the conventional cycle is the air separation unit (ASU), which supplies oxygen at 99.5% purity at a pressure of 120 bar. The pure oxygen, to be sent to the combustion chamber in an overstoichiometric amount of 3%, is at first mixed with a CO₂ stream recirculated from the end of the cycle, obtaining, overall, an oxidant mixture with a molar fraction of 13.34% O₂ [45,46]. This preliminary blending is useful to avoid corrosion problems of the metallic walls of the heat recuperator. This oxidant flow is compressed up to the highest pressure of the cycle and then preheated in a heat recovery unit up to 720 °C to be subsequently fed to the combustion chamber.

The fuel, methane or coal syngas in the conventional cycle [40] and the oxidant are fed in the combustion chamber at a pressure between 200 and 400 bar. A second CO₂ flow is sent to the combustion chamber with the double task of limiting the combustion temperature (to avoid material resistance problems) and obtaining a working fluid (exhaust gas) that is almost completely composed of CO₂, with small percentages of H₂O vapour derived from combustion and some traces of unburned O₂. The resulting temperature of the exhaust gases is about 1150–1200 °C, and it corresponds to the turbine inlet temperature.

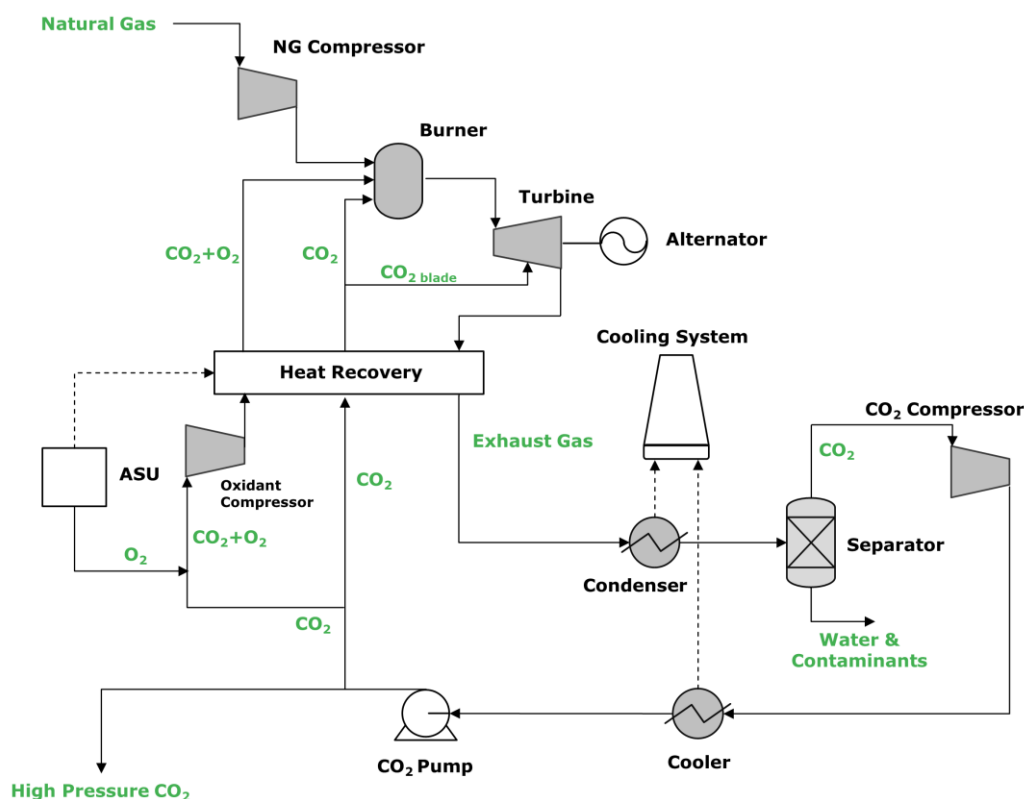


Figure 2. Conventional Allam cycle fueled by natural gas.

The high-pressure gaseous stream leaving the combustion chamber expands in a turbine having an expansion ratio between 6 and 12. The exhaust gases at the turbine outlet, which are at a temperature of about 740 °C and a pressure of 34 bar [45], enter a multi-flow heat exchanger, where they transfer their energy content to various flows for energy recovery purposes. In particular, exhaust gases give part of their thermal energy to the CO₂ flow used as a combustion temperature moderator, to the oxidant flow composed of CO₂ and O₂, and to a third CO₂ flow used as a cooling fluid for the turbine blades.

At the outlet of the heat exchanger, the exhaust gases are cooled down to room temperature, allowing the condensation and the extraction of water vapour to be achieved.

The residual gaseous flow, essentially composed of CO₂, is compressed and cooled in several stages, entering into supercritical state. Finally, it is sent to a multistage centrifugal pump, which again increases its pressure up to that of the combustion chamber.

To close the loop and ensure the mass balance of the CO₂ circulating in the system, it is necessary to extract from the cycle an amount of carbon dioxide equal to the net product derived from the combustion reaction between the fuel and oxygen previously added to the combustion chamber. Thus, as additional output besides electricity, a high-purity, compressed CO₂ flow, is obtained, ready for storage or industrial use. Obviously, CO₂ can be extracted before or after compression, depending on the intended use. The creators of the cycle have estimated that a natural gas-fired power plant with carbon capture based on this technology can achieve theoretical conversion efficiency (on an LHV basis) of around 58.9% (comparable with combined cycle power plants fuelled by natural gas and without CO₂ capture) or about 51.44% if the plant is fed with coal-derived syngas. A 50 MW plant based on the Allam cycle and fuelled by natural gas has already been built and successfully tested in Texas [42], while the construction of a new 300 MW plant is expected to start in 2023 and its full operation in 2026, together with similar announced projects in other locations or countries [42,47]. Since its presentation, the Allam cycle has become a subject of research for academics, who have focused on the thermodynamic analysis of the operating parameters [45,48–50], on new operating modes aimed at increasing plant efficiency [51,52]

or on investigating the integration of a gasifier within the plant to use solid fuels rather than natural gas [53–55].

3. Description of the Proposed Cogeneration Plant

As shown in Figure 3, four fundamental sections compose the proposed system:

- An electrolysis section;
- A gasification section;
- A power section;
- A methanation section.

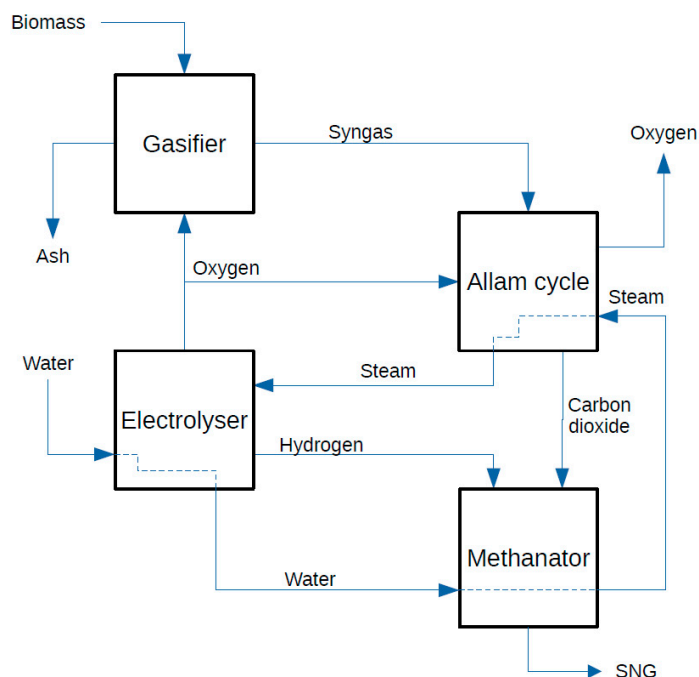


Figure 3. Scheme of the proposed cogeneration plant.

The gasifier is a chemical reactor in which a solid fuel (biomass, in this case) undergoes thermal degradation (pyrolysis) and partial combustion so that it is transformed into a gaseous fuel known as syngas, mainly composed of carbon monoxide and hydrogen, with lower contents of other gaseous substances. The electrolyser is an electrochemical device capable of splitting water into hydrogen and oxygen using electricity. The methanator is a catalytic thermochemical reactor in which carbon dioxide, carbon monoxide and hydrogen can react together to produce methane and water.

Using the power surplus from RESs, a water stream is split into hydrogen and oxygen in the electrolysis section. Water electrolysis can be carried out either at low temperature or at high temperature. In this case, a solid oxide electrolyser (SOEC) working at an average temperature of 800 °C has been selected. The conversion ratio from electric power to hydrogen has been assumed equal to 85%, thanks to the fact that thermal power also contributes to the process. To reduce the compression work, the electrolysis process is carried out at 30 bar. The gases at the outlet of the cell are then cooled, transferring the high-temperature heat to the feed water.

The same pressure has also been adopted for the gasification section, which converts biomass into syngas. A lignocellulosic biomass with negligible quantities of sulphur or chlorine compounds has been selected (Table 1) in order to avoid the need for an acid gas removal unit; however, it is possible to include it in the layout when required. A part of the electrolytic oxygen is used as gasifying agent for the biomass, in order to obtain a syngas with high calorific value and, overall, with a minimum content of nitrogen (deriving from the biomass). The obtained syngas is cooled in a heat regenerator to reduce its temperature

and condense its water content before compression. The highest operating pressure of the Allam cycle selected in this study is 305 bar, so that the syngas is compressed to such a pressure before entering the combustion chamber. In order to save energy, such compression is carried out using four intercooled compressors. Finally, syngas is sent back to the heat regenerator to increase its temperature.

Table 1. Composition and calorific values of the selected biomass [35].

| Proximate Analysis (w%) | | Ultimate Analysis (w%) | |
|-------------------------|------------|------------------------|--------|
| Fixed carbon | 14.89 | C | 50.4 |
| Volatile matter | 64.87 | H | 6.1 |
| Moisture | 20 | N | 0.1 |
| Ash | 0.24 | O | 43.1 |
| | | Ash | 0.3 |
| | LHV | MJ/kg | 12.480 |
| | HHV | MJ/kg | 14.078 |

The power section receives syngas and a stoichiometric amount of oxygen and produces electricity and a flow essentially consisting of water and carbon dioxide, with a few traces of nitrogen, oxygen, carbon monoxide and hydrogen. These traces do not pose purity problems or separation needs, as the captured CO₂ flow is sent to the methanation unit. In the proposed system, syngas is burnt with a stoichiometric amount of oxygen inside the combustion chamber and not with an overstoichiometric amount, as in the original Allam cycle, thus achieving slightly less complete combustion. The stoichiometric oxygen amount was selected in order to obtain a very low oxygen content in the exhaust gas and thus in the captured CO₂ flow, since introducing a higher oxygen content in the methanator would lower the methane yield, while carbon monoxide deriving from incomplete combustion is converted into methane inside the methanator. Being the combustion between syngas and oxygen an oxycombustion, the temperature would be too high for usual materials; therefore, a recycled carbon dioxide stream that acts as a temperature moderator is fed to the combustion chamber. Another effect of this additional flow is to increase the total mass flow rate entering the turbine, thus increasing the mechanical power obtained. A second flow of recycled carbon dioxide is fed to the turbine through its blades in order to cool them. Overall, the gas is expanded in the turbine from the pressure of 305 bar down to 34 bar. The gas resulting from combustion is almost exclusively composed of carbon dioxide, and steam, which can be easily removed by means of cooling and condensation. The resulting gas after water separation is almost pure carbon dioxide and corresponds to the recycled flow plus that generated by means of syngas combustion. In a traditional Allam cycle, after expansion, this last amount could be extracted from the plant and vented into the atmosphere with no environmental impact when the carbon content comes from biomass. However, it could also be captured to obtain a negative carbon footprint; indeed, in the proposed plant, this CO₂ is captured and fed to the methanation section. After expansion, the recycled carbon dioxide flow needs to be recompressed to the Allam cycle higher operating pressure. In this case, the compression is carried out with six intercooled steps, i.e., three compressors and three pumps, since at a pressure higher than 73.8 bar, carbon dioxide becomes liquid or supercritical fluid, depending on the temperature. After compression, the recycled carbon dioxide stream is heated by the gas exiting from the turbine inside a recovery heat exchanger.

The last section, i.e., the methanation unit, receives carbon dioxide from the power section and hydrogen from the electrolysis section. It is based on the Sabatier reaction, and a TREMP layout has been adopted. It consists of a series, three in this case, of adiabatic reactors operating at 30 bar and at gradually reduced temperature. The first reactor receives the flows of carbon dioxide and hydrogen plus a flow recycled upstream of the second

reactor. Such a flow has the goal to control the reaction temperature, which would become too high for catalysts in the absence of methane. The catalysts used by the TREMP process can work in the range of 250–700 °C. No recycling is required by the second and third reactors, since they receive a flow already containing a high percentage of methane. As the reaction is exothermic and the reactors are adiabatic, there is the need to reduce the gas temperature before sending the gas to the next reactor. Therefore, downstream of each reactor, a recovery heat exchanger has been introduced to transfer heat to the water fed to the electrolysis section. Finally, a condenser has also been included downstream of the third reactor with the task to dry the SNG.

4. Model

The proposed system was analysed by means of a simulation carried out using Aspen Plus software. The method used to calculate the properties of the species involved was that of Peng–Robinson [45,46]. First, an Aspen Plus model of the natural gas-fuelled conventional Allam cycle alone was validated against literature data [46]. This model was then slightly modified to consider biomass syngas, instead of natural gas, and electrolytic oxygen, instead of oxygen produced by an ASU, analysing the differences with respect to the conventional model. Finally, this Allam cycle model was integrated with the rest of the proposed plant.

All compressors and pumps were modelled with isentropic efficiency of 0.85 and mechanical efficiency of 0.98. All turbines were modelled with isentropic efficiency of 0.93 and mechanical efficiency of 0.98. The isentropic efficiency of the water pump in the electrolysis section was set to 0.7. No pressure drops were considered for the heat exchangers. All intercoolers were modelled with an exit temperature of 33 °C, with the only exception of the coolers in the Allam cycle before the CO₂ pumps, which were set to 31 °C.

Figure 4 shows the model of the SOEC used in the proposed system.

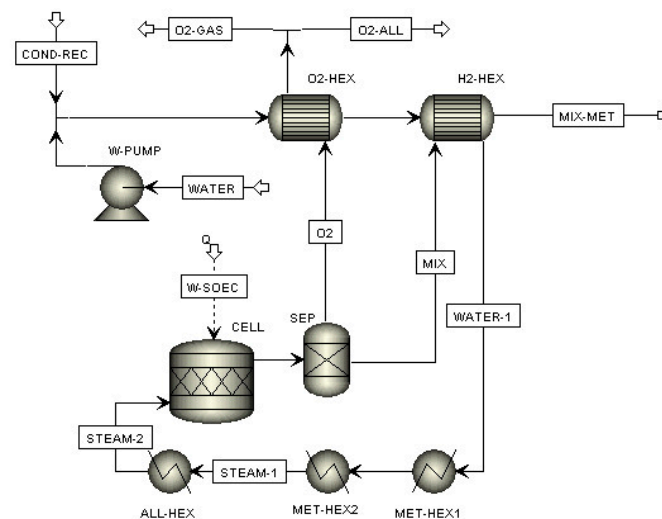


Figure 4. Model of the solid oxide electrolyser section.

The electrolyser was modelled as a stoichiometric reactor performing a 0.85 conversion of the water split reaction (CELL) followed by a separator (SEP). The electric power required for the electrolysis process (W-SOEC) was supplied to the electrolyser as a heat power input. Two flows at 30 bar and 825 °C exit from the separator: oxygen and a mix of hydrogen and residual steam. Both are cooled (O2-HEX and H2-HEX), transferring heat to the feed water, which also receives heat from the methanation (MET-HEX1 and MET-HEX2) and power (ALL-HEX) sections and becomes superheated steam at 775 °C before entering the cathode. The oxygen flow, cooled down to 33 °C, is split in two flows: the first one (O2-GAS) is fed to the biomass gasifier, whereas the second one (O2-ALL) enters the power section. The flow of hydrogen and residual steam (MIX-MET) is fed to the methanation section at 255 °C.

Figure 5 shows the model of the biomass gasifier section. An updraft gasifier was selected in such a way that biomass was directly dried by the syngas exiting from the gasifier. It was modelled as a couple of reactors and separators. The first reactor (DECOMP) is a Yield reactor with the task to decompose biomass in its elementary components plus humidity and ash, as shown in Table 1. This is followed by a separator (WAT-SEP) in which the syngas exiting the gasifier extracts the humidity. The second reactor (GASIF) is a Gibbs reactor fed by the dried flow coming from the separator and by part of the electrolytic oxygen coming from the electrolysis section, so that the biomass undergoes partial oxidation. In the Aspen Plus model, a heat stream connects DECOMP and GASIF in order to achieve an automatic heat balance that takes into account both the enthalpy of decomposition and that of gasification. The gasifier operates at 30 bar and about 800 °C. The syngas produced crosses a separator (ASH-SEP), which removes the ash and finally absorbs the humidity. The syngas needs to be compressed at 305 bar, which is the operating pressure of the Allam cycle. In order to minimise the power consumption, the syngas is first cooled inside a regenerative heat exchanger (R-HEX) down to 190.3 °C and finally in a condenser (GAS-COND), which makes it possible to separate the water. The dry syngas is then supplied to four intercooled compression stages and finally re-enters the regenerative heat exchanger in such a way to recover heat before leaving the gasifier section at 455 °C.

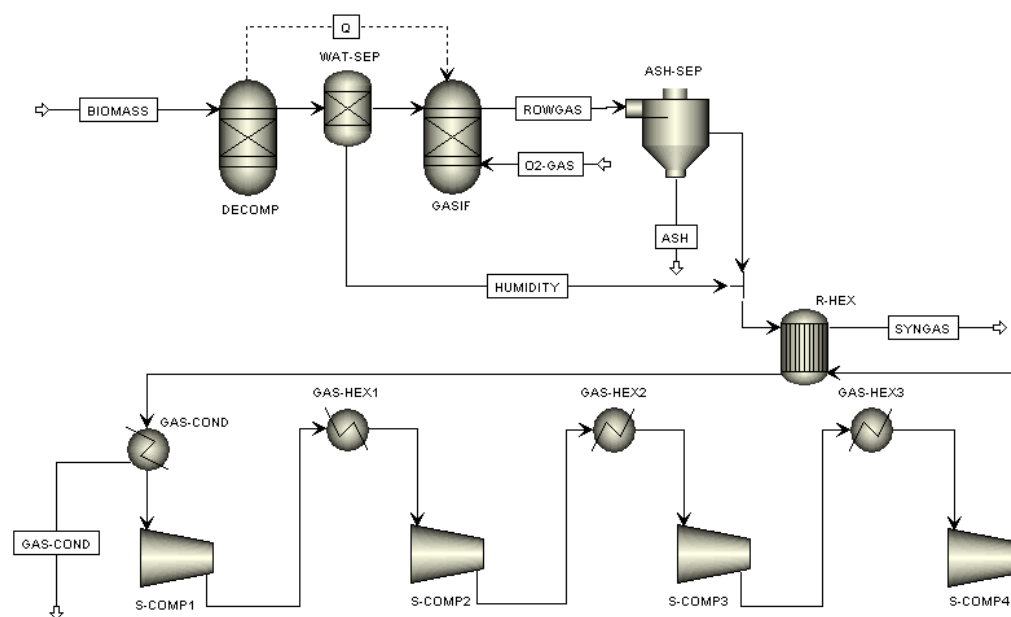


Figure 5. Model of the biomass gasifier section.

The power section was modelled based on an Allam cycle plant (Figure 6), which makes it possible to obtain both mechanical power on the turbine axis for electricity production and an output flow consisting of high-purity carbon dioxide, suitable for being sent to the methanation section for the production of SNG.

The combustion chamber (COMB-CH) was modelled with a Gibbs reactor operating at 305 bar and fed with the syngas coming from the gasifier section (SYNGAS) and the oxygen coming from the electrolysis section (O2-CC). The latter needs to be compressed from 30 bar up to 305 bar, and this has been achieved using three intercooled compressors. A flow of oxygen (O2-STOR) exceeding the amount required by the syngas combustion is separated at 200 bar after the second intercooler; this might be accumulated to be sold, given its high purity.

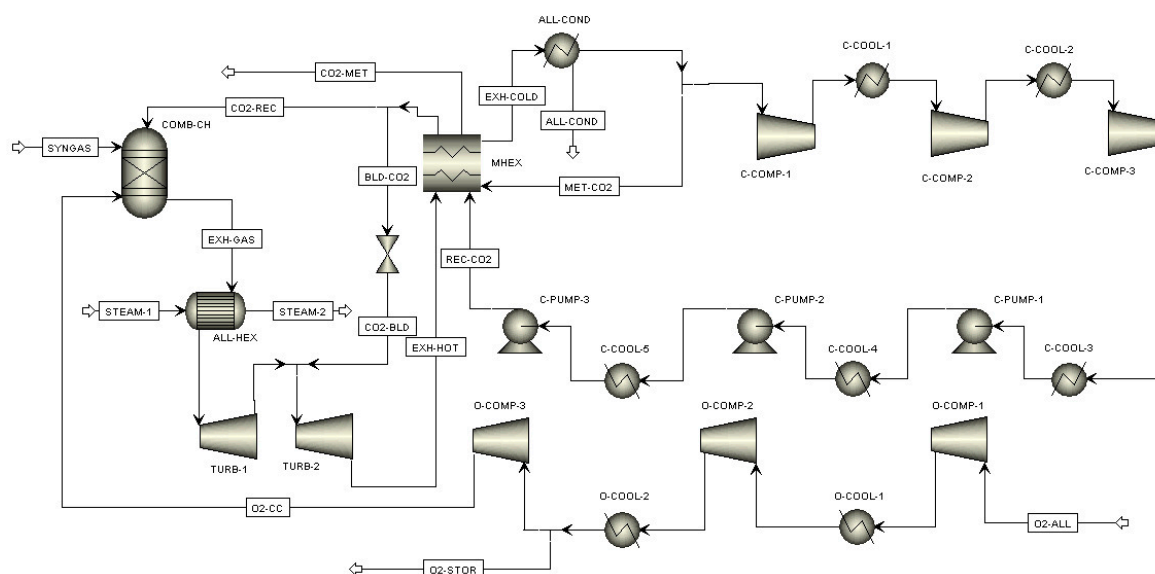


Figure 6. Model of the Allam cycle power section.

The exhaust gas leaving the burner at 1213 °C is supplied to a heat exchanger (ALL-HEX) which receives from the methanation section steam at 582 °C (STEAM-1) which then goes to the electrolyser at 775 °C (STEAM-2). After the heat exchange with steam, exhaust gas enters the turbine at 1150 °C. In addition to the reactants, a temperature moderator consisting of a recycled flow of carbon dioxide (CO₂-REC) at 720 °C is supplied to the combustion chamber in order to obtain a turbine inlet temperature of 1150 °C. The gas turbine also receives further carbon dioxide blown through the turbine blades in order to cool the blades themselves. To simplify the model, a couple of gas turbines (TURB-1 and TURB-2) were utilised with the total cooling flow (CO₂-BLD) at 717 °C added between the two turbines. The cooling flow added is such that the final temperature of the exhaust gas exiting the turbine is 774 °C, approximately the same as in the original Allam cycle.

Therefore, the gas exiting at 34 bar from the turbine (EXH-HOT) is composed of the product of syngas combustion, almost-pure steam and carbon dioxide, and recycled carbon dioxide. Steam has to be condensed. A flow of carbon dioxide corresponding to the combustion product has to be fed to the methanation unit, whereas the residual flow has to be recompressed and recycled.

The first step is the cooling of exhaust gas inside a multi-flux heat exchanger (MHEX), which elaborates three different flows. Then, the exhaust gas (EXH-COLD) at 51.1 °C is sent to a condenser (ALL-COND) to condense and remove water. At this point, the almost-pure carbon dioxide flow is split to separate the carbon dioxide produced during combustion (MET-CO₂), which is heated up to 300 °C inside the above-mentioned multi-flux heat exchanger and supplied to the methanation section (CO₂-MET).

The residual flow (REC-CO₂) is recompressed using three intercooled compressors and three pumps up to the pressure of 305 bar. Then, the flow is heated up to 720 °C inside the above-mentioned multi-flux heat exchanger and finally split to separate the stream for turbine cooling (BLD-CO₂) from the stream sent to the combustion chamber (CO₂-REC).

The part of the plant devoted to the Sabatier process (Figure 7) consists of three adiabatic methanation units operating at 30 bar.

The first consists of a Gibbs reactor (MET1) fed with a flow of electrolytic hydrogen mixed with a residual amount of water (MIX-MET) at 255 °C and with a flow of carbon dioxide extracted at 300 °C from the power section (CO₂-MET). In addition, there is a partial recycling of the outgoing gas (SNG-REC), according to the TREMP layout designed by Haldor Topsoe. The reactor is followed by a countercurrent, two-stream heat exchanger (MET-HEX2) having the task to recover heat from the flow exiting the reactor and transfer it to the steam entering the Allam section (STEAM-1) at 582 °C.

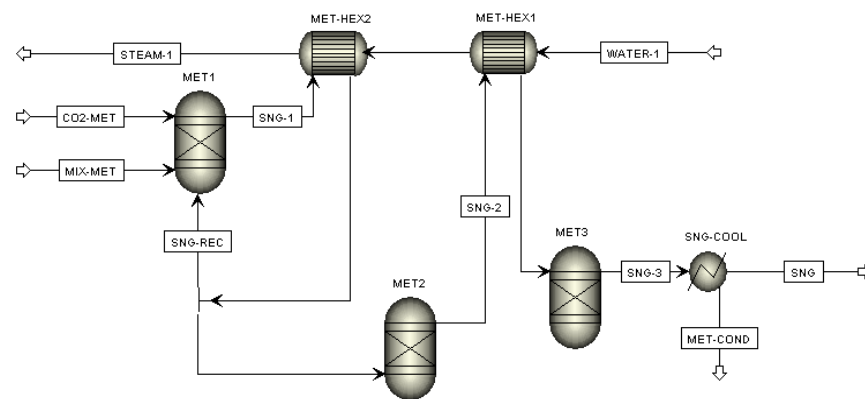


Figure 7. Model of the methanation section for SNG production.

The second unit is almost identical to the first one, with a Gibbs reactor (MET2) and a countercurrent, two-stream heat exchanger (MET-HEX1) having the task to recover heat from the flow exiting the reactor and transfer it to the water coming from the SOEC section (WATER-1). In this case, there is no recycling, and the reactor is only fed with the gas stream from the first unit after splitting for recycling.

Finally, the third unit receives the gas from the second unit. It is composed of a Gibbs reactor (MET3) and a cooler with no heat recovery (SNG-COOL) for the refrigeration and dehumidification of the SNG produced, which mainly consists of methane and is suitable for storage or injection into the natural gas distribution network.

5. Results

A flow rate of 1 kmol/s of water fed to the electrolyser was considered. This corresponded to an input to the gasifier of 6.3 kg/s of the biomass defined in Table 1. The electrolytic oxygen used for gasification (O₂-GAS) amounted to 2.584 kg/s, supplied at 33 °C and 30 bar.

Figure 8 shows a detail of the syngas flows in the gasification section. The biomass is dehumidified by the syngas produced to facilitate the gasification process; therefore, the moisture present in the biomass is found in the syngas (5-SYN4). It is removed by means of condensation, since the syngas is refrigerated (5-SYN6) before being brought to the operating pressure of the Allam cycle. This compression is carried out in four intercooled stages, downstream of which the syngas (5-SYN13) is heated in a regenerative exchanger, countercurrent with respect to the flow leaving the cyclone (5-SYN4). Finally, the resulting syngas is sent to the power unit (5-SYN14).

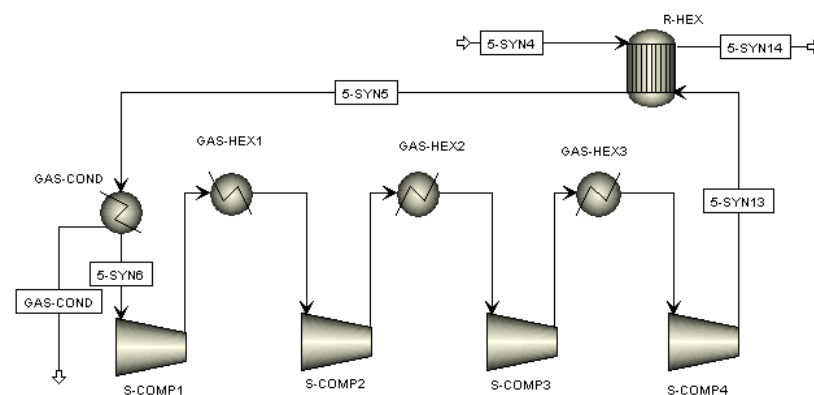


Figure 8. Detail of the syngas flows in the gasification section.

The characteristics of the main syngas flows in the gasification section are shown in Table 2.

Table 2. Characteristics of the main flows of the gasification section.

| Molar Flow (mol/s) | 5-SYN4 | 5-SYN5 | 5-SYN6 | 5-SYN13 | 5-SYN14 |
|--------------------|--------|--------|--------|---------|---------|
| H ₂ O | 108.0 | | 0.6 | | |
| H ₂ | | | 57.2 | | |
| CO | | | 106.6 | | |
| CO ₂ | | | 76.3 | | |
| CH ₄ | | | 28.6 | | |
| N ₂ | | | 0.2 | | |
| Total flow (mol/s) | 376.9 | | 269.4 | | |
| Temperature (°C) | 474.9 | 190.3 | 33.0 | 86.7 | 454.9 |
| Pressure (bar) | 30 | | 305 | | |
| Vapor fraction | 1 | | | | |

The syngas is then fed to the combustion chamber together with a flow of oxygen that comes from the SOEC section. The features of the main flows of the electrolysis section are shown in Table 3. The electrolysis section receives a flow of water (WATER) at room temperature, which, after compression, is mixed with the water recovered from the other sections (COND-REC). This flow is partially evaporated by recovering heat from the products coming out of the electrolyser (O₂ and MIX) and then by completing evaporation and overheating at the expense of the heat recovered from other sections. The flow of hydrogen and residual water (MIX-MET) is sent to the methanation section. The oxygen flow is divided into two flows, where the first (O₂-GAS) is sent to the gasification section, while the second (O₂-ALL) is sent to the Allam section.

Table 3. Characteristics of the main flows of the electrolysis section.

| Molar Flow (mol/s) | WATER | WATER-1 | STEAM-2 | MIX | MIX-MET | O ₂ | O ₂ -GAS | O ₂ -ALL |
|--------------------|--------|---------|---------|--------|---------|----------------|---------------------|---------------------|
| H ₂ O | 1000.0 | | | 150.0 | | 0 | | |
| H ₂ | 0 | | | 850.0 | | 0 | | |
| O ₂ | 0 | | | 0 | | 425.0 | 80.8 | 344.2 |
| Total flow (mol/s) | 1000.0 | | | 1000.0 | | 425.0 | 80.8 | 344.2 |
| Temperature (°C) | 20 | 233.9 | 775.0 | 825.0 | 255.0 | 825.0 | 33.0 | |
| Pressure (bar) | 30 | | | | | | | |
| Vapor fraction | 0 | 0.398 | | | | 1 | | |
| Liquid fraction | 1 | 0.602 | | | | 0 | | |

The latter flow exceeds the flow rate required by the burner; therefore, it is split in two streams after being compressed to 200 bar. This first compression is carried out with a couple of intercooled compressors. After the second cooling process, the exceeding flow (O₂-STOR) is separated; it may be available for selling or for other applications. The remaining flow is finally compressed to 305 bar and fed (O₂-CC) to the combustion chamber.

The features of the main flows of the Allam section are shown in Tables 4 and 5. The burnt gas from the combustion chamber (EXH-GAS) enter the heat exchanger (ALL-HEX) and then the gas turbine, whose blades are cooled by a carbon dioxide flow (CO₂-BLD). After expansion down to 34 bar, the gas flow (EXH-HOT) at 774 °C enters the multi-flux heat exchanger and leaves it at 51.1 °C (EXH-COLD). With further cooling to 33 °C, almost all steam is condensed and separated (ALL-COND).

After condensation, the almost-pure stream of carbon dioxide is split into two flows. The first one (MET-CO₂) corresponds to the product of combustion and is sent to the multi-flux heat exchanger, from which it exits at 300 °C (CO₂-MET) to be fed to the methanation section. The captured CO₂ flow that is sent to methanation presents a purity of 99.67%. The second flow (REC-CO₂) corresponds to the recirculation flow and is recompressed to 305 bar. After recompression, the flow is sent to the multi-flux heat exchanger to be heated up to 720 °C and is finally split to be sent to the combustion chamber (CO₂-REC) to moderate the temperature and to the turbine (CO₂-BLD) for blades cooling.

Table 4. Main oxygen, exhaust gas and condensed water flows of the Allam section.

| Molar Flow (mol/s) | O2-STOR | O2-CC | EXH-GAS | EXH-HOT | EXH-COLD | ALL-COND |
|--------------------|---------|-------|---------|---------|----------|----------|
| H ₂ O | 0 | | 119.0 | 119.1 | | 114.5 |
| H ₂ | traces | | | | | |
| O ₂ | 205.1 | 139.1 | | traces | | |
| CO | 0 | | | 0.2 | | 0 |
| CO ₂ | 0 | | 2038.5 | 2076.0 | | 0 |
| N ₂ | 0 | | | 2 | | 0 |
| Total flow (mol/s) | 205.2 | 139.1 | 2156.1 | 2193.5 | | 114.5 |
| Temperature (°C) | 33.0 | 76.4 | 1212.7 | 774.0 | 51.1 | 33.0 |
| Pressure (bar) | 200 | 305 | | 34 | | |
| Vapor fraction | | 1 | | | 0.951 | 0 |
| Liquid fraction | | 0 | | | 0.049 | 1 |

Table 5. Main carbon dioxide flows of the Allam section.

| Molar Flow (mol/s) | MET-CO2 | CO2-MET | REC-CO2 | CO2-BLD | CO2-REC |
|--------------------|---------|---------|---------|---------|---------|
| H ₂ O | 0.5 | | 4.2 | 0.1 | 4.1 |
| H ₂ | traces | | | | |
| O ₂ | traces | | | | |
| CO | 0.2 | | | | |
| CO ₂ | 211.4 | | 1864.4 | 37.3 | 1827.1 |
| N ₂ | 0.2 | | 1.6 | traces | 1.6 |
| Total flow (mol/s) | 212.1 | | 1870.4 | 37.4 | 1832.8 |
| Temperature (°C) | 33 | 300 | 43.3 | 717.4 | 720 |
| Pressure (bar) | 34 | | 305 | 100 | 305 |
| Vapor fraction | 1 | | | | |
| Liquid fraction | 0 | | | | |

The features of the main flows of the methanation section are shown in Table 6. The stream of hydrogen (and water) coming from the electrolysis section (MIX-MET) and that of carbon dioxide coming from the Allam section (CO2-MET) are fed to the first methanation reactor together with the recycled SNG flow (SNG-REC). The product gas (SNG-1) exits from the first reactor at 606.3 °C with a methane concentration of about 18.5%. After refrigeration down to about 300 °C and splitting for recycling, the gas is fed to the second reactor, which increases the methane concentration up to about 23.5% and the temperature to 467.5 °C (SNG-2). After a new refrigeration process, the gas is fed to the third reactor for the final conversion. The methane concentration reaches the value of 26.1% (SNG-3), which is not very high due to the significant formation of water during the methanation process. The final cooling down to 33 °C allows to condensate and separate almost all water (MET-COND), so that the composition of the SNG results to be 89.2% CH₄, 8.8% H₂, 1.7% CO₂, 0.2% H₂O and 0.1% N₂ (LHV = 48.072 MJ/kg; HHV = 53.466 MJ/kg). The obtained SNG flow rate resulted to be 3.56 kg/s. The sequence of SNG composition obtained downstream of each methanation reactor and after final drying is graphically shown in Figure 9.

Table 6. Characteristics of the main flows of the methanation section.

| Molar Flow (mol/s) | SNG-1 | SNG-REC | SNG-2 | SNG-3 | SNG | MET-COND |
|--------------------|--------|---------|-------|--------|-------|----------|
| H ₂ O | 1211.4 | 726.8 | 539.0 | 565.2 | 0.5 | 564.7 |
| H ₂ | 470.4 | 282.2 | 74.0 | 20.4 | | 0 |
| CO | 15.8 | 9.5 | 0.4 | traces | | 0 |
| CO ₂ | 103.0 | 61.9 | 17.2 | 4.1 | | 0 |
| CH ₄ | 409.7 | 245.8 | 193.9 | 207.4 | | 0 |
| N ₂ | 0.5 | 0.3 | | 0.2 | | 0 |
| Total flow (mol/s) | 2210.9 | 1326.5 | 824.3 | 797.3 | 232.6 | 564.7 |
| Temperature (°C) | 606.3 | 305.0 | 467.5 | 333.2 | 33.0 | |
| Pressure (bar) | 30 | | | | | |
| Vapor fraction | 1 | | | | | 0 |
| Liquid fraction | 0 | | | | | 1 |

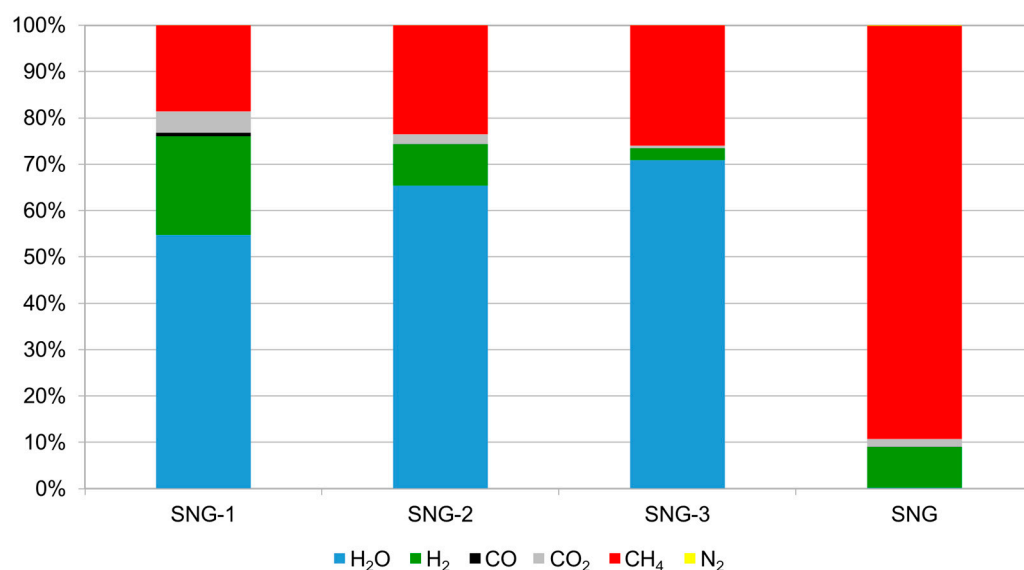


Figure 9. Sequence of the obtained SNG composition.

Finally, the global energy balance is reported in Table 7. The electrolysis section required an input of 222.398 MW as electric power for electrolysis, plus the thermal power input recovered from other sections and 0.016 MW of mechanical power for the water pump.

Table 7. Global energy balance of the proposed system.

| | Input | Output |
|---------------------------|---------|---------|
| Chemical power (MW) | 78.625 | 170.805 |
| Electric power (MW) | 222.398 | 32.677 |
| Total power (MW) | 301.023 | 203.482 |
| Efficiency, LHV basis (%) | | 67.60 |
| Efficiency, HHV basis (%) | | 71.57 |

The gasification section required an input of 1.995 MW as mechanical power for gas compression and an input of 78.625 MW as chemical power of the biomass consumed. The turbines in the Allam section produced 45.343 MW, while the CO₂ and the O₂ compression lines required 7.653 MW and 2.503 MW of mechanical power, respectively. Overall, the Allam section required chemical power coming from the gasification section and generated 35.186 MW of net mechanical power. By also taking into consideration the mechanical power required by the water pump and the gasification section, the net mechanical power produced by the whole plant was 33.174 MW. Assuming an electric efficiency value of 0.985, the electric power generated was 32.677 MW.

Finally, the methanation section required an input of chemical power corresponding to the hydrogen produced by the electrolysis section and generated a chemical power of 170.805 MW, based on LHV, or 189.970 MW, based on HHV, as SNG. It is possible to calculate the overall plant efficiency as shown in the following equation:

$$\eta_{\text{plant}} = \frac{\dot{m}_{\text{SNG}} \cdot \text{HHV}_{\text{SNG}} + \text{Electricity}_{\text{out}}}{\dot{m}_{\text{biomass}} \cdot \text{HHV}_{\text{biomass}} + \text{Electricity}_{\text{in}}} \quad (1)$$

The results show global plant efficiency of 67.60% on an LHV basis and 71.57% on an HHV basis. Finally, this paper mainly deals with the proof of concept and with the integration of the various sections of the plant. Future studies should focus on the sizing of the proposed system to a size compatible with the coupling with RES plants (especially regarding the electrolyser) and the further optimization of the various plant sections. Nevertheless, different types of input biomass or of synthetic fuels and green chemicals as

outputs could be explored, while the environmental suitability could be checked using a life-cycle approach.

6. Conclusions

This paper proposes a novel integrated system for the cogeneration of electricity and the simultaneous production of substitute natural gas, starting from lignocellulosic biomass, water and renewable electricity. Through the production of renewable fuel, this system could serve as energy storage, helping to increase the flexibility and interconnection of natural gas and electricity grids as well as the share of renewable sources in the energy mix. The main novelty of this study lies in the coupling of a power unit based on the Allam thermodynamic cycle with a water electrolyser, a biomass gasifier and a methanation section. The Allam power cycle uses supercritical CO₂ as evolving fluid and is based on the oxycombustion, of a biomass syngas in this case, allowing carbon dioxide capture and utilisation to be more easily achieved. Electrolytic oxygen can be valorised and used for oxycombustion, while the CO₂ captured from the power cycle (simply by means of water condensation) can be used for the production of renewable fuel (SNG in this case). In addition, electricity is simultaneously produced by the power cycle with better programmability and continuity than wind or solar power. The results show an efficiency value of the proposed system of around 68% on an LHV basis, producing almost 33 MW of net electrical power and 171 MW of SNG chemical power, against an energy input of 222 MW renewable electricity and 78.6 MW of biomass. The composition of the produced SNG showed contents of 89.2% CH₄ and 8.8% H₂, resulting in a gas with high calorific value that could be injected into the existing natural gas grid. The current barriers to the injection of SNG with similar composition in the natural gas grid are mostly of legislative rather than technical nature. However, higher methane contents could also be obtained by means of the further optimisation of the methanation section. For realistic coupling with renewable energy sources, it would be essential to scale the system to a size compatible with those of common wind and photovoltaic plants. Future studies could explore the further optimisation of the plant and waste heat recovery, the use of different types of biomass, the coupling of anaerobic digestion systems with the Allam cycle and the production of different fuels, such as methanol. Finally, an analysis of the environmental impacts (for example, through life-cycle assessment) would be crucial to evaluate the environmental sustainability of the gas produced compared with conventional systems.

Author Contributions: Conceptualization, D.C. and G.S.; Methodology, D.C. and G.S.; Software, G.S.; Validation, D.C.; Formal analysis G.S. and D.C.; Investigation, D.C.; Resources, G.S.; Data curation G.S., D.C.; Writing—original draft preparation, D.C.; Writing—review and editing, G.S.; Visualization, G.S.; Supervision, G.S.; Project administration, G.S.; Funding acquisition, G.S. All authors have read and agreed to the published version of the manuscript.

Funding: This research received no external funding.

Data Availability Statement: All relevant data to reproduce the study are already available in this article. Further data sharing is not applicable to this article.

Conflicts of Interest: The authors declare no conflict of interest.

References

1. IPCC Global Warming of 1.5 °C: An IPCC Special Report on the Impacts of Global Warming of 1.5°C above Pre-Industrial Levels and Related Global Greenhouse Gas Emission Pathways, in the Context of Strengthening the Global Response to the Threat of Climate Change, Sustainable Development, and Efforts to Eradicate Poverty; Intergovernmental Panel on Climate Change; Masson-Delmotte, V., Zhai, P., Pörtner, H.-O., Roberts, D., Skea, J., Shukla, P.R., Pirani, A., Moufouma-Okia, W., Péan, C., Pidcock, R., et al., Eds. Cambridge University Press: Cambridge, UK; New York, NY, USA, 2019; Available online: https://www.ipcc.ch/site/assets/uploads/sites/2/2019/06/SR15_Full_Report_High_Res.pdf (accessed on 12 December 2022). [CrossRef]
2. IPCC Climate Change 2022: Impacts, Adaptation and Vulnerability; Contribution of Working Group II to the Sixth Assessment Report of the Intergovernmental Panel on Climate Change; Pörtner, H.-O., Roberts, D.C., Tignor, M., Poloczanska, E., Mintenbeck, K., Alegría, A., Craig, M., Langsdorf, S., Lösschke, S., Möller, V., et al., Eds. Cambridge University Press: Cambridge, UK, 2022.

3. UNFCCC Adoption of the Paris Agreement; United Nations Framework Convention on Climate Change: Paris, France, 2015.
4. European Commission European Green Deal: Commission Proposes Transformation of EU Economy and Society to Meet Climate Ambitions. Available online: https://ec.europa.eu/commission/presscorner/detail/en/IP_21_3541 (accessed on 14 July 2021).
5. U.S. Department of Energy DOE Industrial Decarbonization Roadmap. Available online: <https://www.energy.gov/eere/industrial-decarbonization-roadmap> (accessed on 7 January 2023).
6. Nasa Earth Observatory Global Patterns of Carbon Dioxide. Available online: <https://earthobservatory.nasa.gov/images/82142/global-patterns-of-carbon-dioxide> (accessed on 5 January 2023).
7. IPCC Climate Change 2013: The Physical Science Basis. Contribution of Working Group I to the Fifth Assessment Report of the Intergovernmental Panel on Climate Change; Stocker, T.F., Qin, D., Plattner, G.-K., Tignor, M., Allen, S.K., Boschung, J., Nauels, A., Xia, Y., Bex, V., Midgley, P.M., Eds. Cambridge University Press: Cambridge, UK; New York, NY, USA, 2013; ISBN 978-1-107-66182-0.
8. Ritchie, H.; Roser, M. Global Greenhouse Gas Emissions by Sector. Available online: <https://ourworldindata.org/emissions-by-sector> (accessed on 27 February 2021).
9. Climate Watch Greenhouse Gas (GHG) Emissions—Historical GHG Emissions by Sector. Available online: https://www.climatewatchdata.org/ghg-emissions?breakBy=sector&end_year=2019&source=ClimateWatch&start_year=1990 (accessed on 5 January 2023).
10. IEA Global Energy Review: CO₂ Emissions in 2021—Global Emissions Rebound Sharply to Highest Ever Level; International Energy Agency: Paris, France, 2022.
11. IEA World Energy Outlook 2022; International Energy Agency: Paris, France, 2022.
12. IEA Renewables 2022—Analysis and Forecast to 2027; International Energy Agency: Paris, France, 2022.
13. IRENA Renewable Capacity Statistics 2022; International Renewable Energy Agency: Abu Dhabi, United Arab Emirates, 2022; ISBN 978-92-9260-428-8.
14. Shafiul Alam, M.; Al-Ismail, F.S.; Salem, A.; Abido, M.A. High-level penetration of renewable energy sources into grid utility: Challenges and solutions. *IEEE Access* **2020**, *8*, 190277–190299. [[CrossRef](#)]
15. Saha, S.; Saleem, M.; Roy, T. Impact of high penetration of renewable energy sources on grid frequency behaviour. *Int. J. Electr. Power Energy Syst.* **2023**, *145*, 108701. [[CrossRef](#)]
16. Dalala, Z.; Al-Omari, M.; Al-Addous, M.; Bdour, M.; Al-Khasawneh, Y.; Alkasrawi, M. Increased renewable energy penetration in national electrical grids constraints and solutions. *Energy* **2022**, *246*, 123361. [[CrossRef](#)]
17. Zhang, Z.; Ding, T.; Zhou, Q.; Sun, Y.; Qu, M.; Zeng, Z.; Ju, Y.; Li, L.; Wang, K.; Chi, F. A review of technologies and applications on versatile energy storage systems. *Renew. Sustain. Energy Rev.* **2021**, *148*, 111263. [[CrossRef](#)]
18. Blanco, H.; Faaij, A. A review at the role of storage in energy systems with a focus on power to gas and long-term storage. *Renew. Sustain. Energy Rev.* **2018**, *81*, 1049–1086. [[CrossRef](#)]
19. Candelaresi, D.; Spazzafumo, G. Introduction: The power-to-fuel concept. In *Power to Fuel—How to Speed Up a Hydrogen Economy*; Spazzafumo, G., Ed.; Academic Press: Cambridge, MA, USA, 2021; pp. 1–15. [[CrossRef](#)]
20. Schaaf, T.; Grünig, J.; Schuster, M.R.; Rothenfluh, T.; Orth, A. Methanation of CO₂-storage of renewable energy in a gas distribution system. *Energy Sustain. Soc.* **2014**, *4*, 2. [[CrossRef](#)]
21. Mazza, A.; Bompard, E.; Chicco, G. Applications of power to gas technologies in emerging electrical systems. *Renew. Sustain. Energy Rev.* **2018**, *92*, 794–806. [[CrossRef](#)]
22. Dahiru, A.R.; Vuokila, A.; Huuhtanen, M. Recent development in Power-to-X: Part I—A review on techno-economic analysis. *J. Energy Storage* **2022**, *56*, 105861. [[CrossRef](#)]
23. Candelaresi, D.; Spazzafumo, G. Power-to-fuel potential market. In *Power to Fuel—How to Speed Up a Hydrogen Economy*; Spazzafumo, G., Ed.; Academic Press: Cambridge, MA, USA, 2021; pp. 239–265. [[CrossRef](#)]
24. Wulf, C.; Zapp, P.; Schreiber, A. Review of Power-to-X demonstration projects in Europe. *Front. Energy Res.* **2020**, *8*, 191. [[CrossRef](#)]
25. Rezazadeh, F. Sector Coupling & Power-to-X Technologies—Shaping an Integrated Green Energy System. Available online: <https://ingenuity.siemens.com/2019/08/sector-coupling-power-to-x-technologies-shaping-an-integrated-green-energy-system/> (accessed on 7 January 2023).
26. Dincer, I. Green methods for hydrogen production. *Int. J. Hydrogen Energy* **2011**, *37*, 1954–1971. [[CrossRef](#)]
27. Melaina, M.W.; Antonia, O.; Penev, M. *Blending Hydrogen into Natural Gas Pipeline Networks: A Review of Key Issues*; National Renewable Energy Laboratory: Golden, CO, USA, 2013. [[CrossRef](#)]
28. IEA The Future of Hydrogen—Seizing Today's Opportunities—Report Prepared for the G20, Japan; International Energy Agency: Paris, France, 2019.
29. Snam Snam: Hydrogen Blend Doubled to 10% in Contursi Trial. Available online: https://www.snam.it/en/Media/news_events/2020/Snam_hydrogen_blend_doubled_in_Contursi_trial.html (accessed on 25 November 2020).
30. Bargiacchi, E.; Candelaresi, D.; Spazzafumo, G. Power to methane. In *Power to Fuel—How to Speed Up a Hydrogen Economy*; Spazzafumo, G., Ed.; Academic Press: Cambridge, MA, USA, 2021; pp. 75–101. [[CrossRef](#)]
31. Götz, M.; Lefebvre, J.; Mörs, F.; McDaniel Koch, A.; Graf, F.; Bajohr, S.; Reimert, R.; Kolb, T. Renewable Power-to-Gas: A technological and economic review. *Renew. Energy* **2016**, *85*, 1371–1390. [[CrossRef](#)]
32. Koj, J.C.; Wulf, C.; Zapp, P. Environmental impacts of power-to-X systems—A review of technological and methodological choices in Life Cycle Assessments. *Renew. Sustain. Energy Rev.* **2019**, *112*, 865–879. [[CrossRef](#)]

33. Stanger, R.; Wall, T.; Spörl, R.; Paneru, M.; Grathwohl, S.; Weidmann, M.; Scheffknecht, G.; McDonald, D.; Myöhänen, K.; Ritvanen, J.; et al. Oxyfuel combustion for CO₂ capture in power plants. *Int. J. Greenh. Gas Control.* **2015**, *40*, 55–125. [CrossRef]
34. Basile, A.; Gugliuzza, A.; Iulianelli, A.; Morrone, P. Membrane technology for carbon dioxide (CO₂) capture in power plants. In *Advanced Membrane Science and Technology for Sustainable Energy and Environmental Applications*; Elsevier: Amsterdam, The Netherlands, 2011; pp. 113–159. [CrossRef]
35. Spazzafumo, G. Storing renewable energies in a substitute of natural gas. *Int. J. Hydrogen Energy* **2016**, *41*, 19492–19498. [CrossRef]
36. Spazzafumo, G. Cogeneration of power and substitute of natural gas using electrolytic hydrogen, biomass and high temperature fuel cells. *Int. J. Hydrogen Energy* **2018**, *43*, 11811–11819. [CrossRef]
37. Frigo, S.; Spazzafumo, G. Comparison of different system layouts to generate a substitute of natural gas from biomass and electrolytic hydrogen. *Int. J. Hydrogen Energy* **2020**, *45*, 26166–26178. [CrossRef]
38. Bargiacchi, E.; Candelaresi, D.; Valente, A.; Spazzafumo, G.; Frigo, S. Life Cycle Assessment of Substitute Natural Gas production from biomass and electrolytic hydrogen. *Int. J. Hydrogen Energy* **2021**, *46*, 35974–35984. [CrossRef]
39. Allam, R.J.; Palmer, M.; Brown, G.W. System and Method for High Efficiency Power Generation Using a Carbon Dioxide Circulating Working Fluid. U.S. Patent US 2011/0179799A1, 28 July 2011. Available online: <http://www.google.com/patents/US20110179799> (accessed on 7 January 2023).
40. Allam, R.J.; Palmer, M.R.; Brown, G.W.; Fetvedt, J.; Freed, D.; Nomoto, H.; Itoh, M.; Okita, N.; Jones, C. High efficiency and low cost of electricity generation from fossil fuels while eliminating atmospheric emissions, including carbon dioxide. *Energy Procedia* **2013**, *37*, 1135–1149. [CrossRef]
41. Allam, R.J.; Fetvedt, J.E.; Forrest, B.A.; Freed, D.A. The Oxy-Fuel, Supercritical CO₂ Allam Cycle: New Cycle Developments To Produce Even Lower-Cost Electricity From Fossil Fuels Without Atmospheric Emissions. In Proceedings of the ASME Turbo Expo 2014: Turbine Technical Conference and Exposition (GT2014), Düsseldorf, Germany, 16–20 June 2014. [CrossRef]
42. Allam, R.; Martin, S.; Forrest, B.; Fetvedt, J.; Lu, X.; Freed, D.; Brown, G.W.; Sasaki, T.; Itoh, M.; Manning, J. Demonstration of the Allam cycle: An update on the development status of a high efficiency supercritical carbon dioxide power process employing full carbon capture. *Energy Procedia* **2017**, *114*, 5948–5966. [CrossRef]
43. Martin, S.; Forrest, B.; Rafati, N.; Lu, X.; Fetvedt, J.; McGroddy, M.; Brown, B.; Allam, R.; Beauchamp, D.; Freed, D. Progress Update On The Allam Cycle: Commercialization Of Net Power And The Net Power Demonstration Facility. In Proceedings of the 14th International Conference on Greenhouse Gas Control Technologies, GHGT-14, Melbourne, Australia, 21–26 October 2018. [CrossRef]
44. Allam, R.J.; Forrest, B.A.; Fetvedt, J.E. Method and System for Power Production with Improved Efficiency. U.S. Patent 10711695B2, 14 July 2020. Available online: <https://patents.google.com/patent/US10711695B2/en> (accessed on 7 January 2023).
45. Scaccabarozzi, R.; Gatti, M.; Martelli, E. Thermodynamic analysis and numerical optimization of the NET Power oxy-combustion cycle. *Appl. Energy* **2016**, *178*, 505–526. [CrossRef]
46. IEAGHG. *Oxy-Combustion Turbine Power Plants*; IEAGHG: Cheltenham, UK, 2015; Available online: https://ieaghg.org/docs/General_Docs/Reports/2015-05.pdf (accessed on 3 January 2023).
47. Powermag NET Power’s First Allam Cycle 300-MW Gas-Fired Project Will Be Built in Texas. Available online: <https://www.powermag.com/net-powers-first-allam-cycle-300-mw-gas-fired-project-will-be-built-in-texas/> (accessed on 3 January 2023).
48. Penkuhn, M.; Tsatsaronis, G. Exergy Analysis of the Allam Cycle. In Proceedings of the 5th International Symposium—Supercritical CO₂ Power Cycles, San Antonio, TX, USA, 28–31 March 2016; Available online: <https://sco2symposium.com/papers2016/OxyFuel/040paper.pdf> (accessed on 3 January 2023).
49. Scaccabarozzi, R.; Gatti, M.; Martelli, E. Thermodynamic optimization and part-load analysis of the NET power cycle. *Energy Procedia* **2017**, *114*, 551–560. [CrossRef]
50. Wimmer, K.; Sanz, W. Optimization and comparison of the two promising oxy-combustion cycles NET Power cycle and Graz Cycle. *Int. J. Greenh. Gas Control.* **2020**, *99*, 103055. [CrossRef]
51. Mitchell, C.; Avagyan, V.; Chalmers, H.; Lucquiaud, M. An initial assessment of the value of Allam cycle power plants with liquid oxygen storage in future GB electricity system. *Int. J. Greenh. Gas Control.* **2019**, *87*, 1–18. [CrossRef]
52. Zhu, Z.; Chen, Y.; Wu, J.; Zhang, S.; Zheng, S. A modified Allam cycle without compressors realizing efficient power generation with peak load shifting and CO₂ capture. *Energy* **2019**, *174*, 478–487. [CrossRef]
53. Lu, X.; Forrest, B.; Martin, S.; Fetvedt, J.; McGroddy, M.; Freed, D. Integration and Optimization of Coal Gasification Systems With a Near-Zero Emissions Supercritical Carbon Dioxide Power Cycle. In Proceedings of the ASME Turbo Expo 2016: Turbomachinery Technical Conference and Exposition, Seoul, Republic of Korea, 13–17 June 2016. [CrossRef]
54. Lu, X.; Beauchamp, D.; Laumb, J.; Stanislawski, J.; Swanson, M.; Dunham, D.; Martin, C. Coal drying study for a direct syngas fired supercritical CO₂ cycle integrated with a coal gasification process. *Fuel* **2019**, *251*, 636–643. [CrossRef]
55. Zhu, Z.; Chen, Y.; Wu, J.; Zheng, S.; Zhao, W. Performance study on s-CO₂ power cycle with oxygen fired fuel of s-water gasification of coal. *Energy Convers. Manag.* **2019**, *199*, 112058. [CrossRef]

Disclaimer/Publisher’s Note: The statements, opinions and data contained in all publications are solely those of the individual author(s) and contributor(s) and not of MDPI and/or the editor(s). MDPI and/or the editor(s) disclaim responsibility for any injury to people or property resulting from any ideas, methods, instructions or products referred to in the content.